Localization of spinons in random Majumdar-Ghosh chains

Arthur Lavarélo[1,*] and Guillaume Roux[1,†]

[1]*Laboratoire de Physique Théorique et Modèles statistiques, Université Paris-Sud, CNRS, UMR8626, 91405 Orsay, France.*

(Dated: September 14, 2012)

We study the effect of disorder on frustrated dimerized spin-$1/2$ chains at the Majumdar-Ghosh point. The Majumdar-Ghosh condition is first generalized in the presence of random bonds, defining a random Majumdar-Ghosh (RMG) point with locally correlated disorder. Using variational methods and density-matrix renormalization group approaches, we show that spinons, the deconfined fractional elementary excitations of the chains, remain gapped at the RMG point but get localized in Lifshitz states whose localization length is analytically obtained. Increasing the disorder strength at the RMG point induces a transition to a paramagnetic phase of localized spinons. Moving away from the RMG point by uncorrelating the random bonds, an effective interaction between spinons brings the chain into a gapless and partially polarized phase for arbitrarily small disorder.

PACS numbers: 75.10.Kt, 75.40.Mg, 75.10.Jm, 75.10.Pq

Spinons are fractional excitations corresponding to half of a spin excitation in quantum magnets. They typically appear in understanding the excitation spectrum of one-dimensional systems such as the frustrated $J_1 - J_2$ Heisenberg chain. This model possesses an exact ground-state at the Majumdar-Ghosh (MG) point $J_1 = 2J_2$ [1] which is the prototype of a valence bond solid (VBS) state and for which a variational approach describes well elementary excitations [2]. Further, spinons play a crucial role in unconventional two-dimensional phase transitions in which they could be deconfined [3]. Investigating the effect of disorder on their dynamics is essential, all the more since randomness is inherent to experimental samples. Possible strategies to study random quantum magnets are bosonization [4], provided the clean system is gapless and the disorder is small, or real-space renormalization group (RSRG) [5], suited for the strong disorder regime. The latter is asymptotically exact in the case of an infinite-disorder fixed point [6], but its outcome can be questioned at small disorder when it converges to a finite-disorder fixed point. Numerical approaches are challenging due to strong finite-size effects from rare events [7]. Unfortunately, the interplay between frustration and disorder cannot be addressed using the powerful quantum Monte-Carlo method because of the sign problem. Lastly, most studies on random magnets focus on the ground-state while little is known about the fate of elementary excitations. So far, the ground-state physics of random frustrated dimerized chains has only been addressed within the RSRG picture [8] and has been found to belong to the class of the large-spin phase [9].

In this Letter, we unveil some remarkable effects of randomness on frustrated dimerized chains using a variational approach supported by density-matrix renormalization group (DMRG) calculations [10]. They provide both quantitative predictions and an intuitive picture of the physics. The analysis follows two steps. First, the Majumdar-Ghosh condition is generalized to random couplings leading to a locally correlated disorder condition dubbed as the random Majumdar-Ghosh (RMG) point. There, an Anderson model governs the dynamics of a spinon which leads to its localization. Increasing disorder, a transition to a paramagnetic phase of localized spinons is found. Moving away from the RMG point by uncorrelating the couplings generates an effective interaction between spinons which stabilizes the formation of domains and leads to the destruction of the spin gap.

The RMG point – We consider a frustrated dimerized spin-$1/2$ chain with random nearest-neighbor couplings α_i and next-nearest neighbor couplings β_i:

$$\mathcal{H} = \sum_i \alpha_i \mathbf{S}_i \cdot \mathbf{S}_{i+1} + \beta_i \mathbf{S}_{i-1} \cdot \mathbf{S}_{i+1} \ , \qquad (1)$$

where $\mathbf{S}_i$ are spin-$1/2$ operators. In the following, the average couplings are written $\overline{\alpha_i} = \alpha$ and $\overline{\beta_i} = \beta$ with $\alpha = 2\beta$ to start from the MG point. Applying $\mathcal{H}$ on the MG state $|\mathrm{MG}\rangle = |\cdots\bullet\!\!-\!\!\bullet\ \bullet\!\!-\!\!\bullet\ \bullet\!\!-\!\!\bullet\ \bullet\!\!-\!\!\bullet\ \bullet\!\!-\!\!\bullet\ \bullet\cdots\rangle$ with dimers $|\bullet\!\!-\!\!\bullet\rangle = \frac{1}{\sqrt{2}}[|\uparrow\downarrow\rangle - |\downarrow\uparrow\rangle]$ starting on even sites $2j$ gives

$$\mathcal{H}|\mathrm{MG}\rangle = \frac{1}{4}\sum_j \left(-3\alpha_{2j} + \alpha_{2j+1} - \beta_{2j} - \beta_{2j+1}\right)|\mathrm{MG}\rangle + \frac{1}{2}\sum_j \left(\alpha_{2j-1} - \beta_{2j} - \beta_{2j-1}\right)|2j-2, 2j+1\rangle \ ,$$

where we write $|2j-2, 2j+1\rangle = |\cdots\bullet\!\!-\!\!\bullet\ \bullet\!\!-\!\!\bullet\ \overset{\frown}{\bullet\!\!-\!\!\bullet}\ \bullet\!\!-\!\!\bullet\ \bullet\cdots\rangle$, the state with a dimer on bond $(2j-2, 2j+1)$. A similar expression is obtained for the other MG state. Thus, MG states remain degenerate eigenstates of the Hamiltonian provided

$$\alpha_i = \beta_i + \beta_{i+1} \quad \text{(RMG condition)} \ , \qquad (2)$$

which is a generalization of the MG point in the random case. It imposes a local correlation between the random couplings. To understand the nature of the ground-state of Hamiltonian (1), we first investigate the elementary spinon excitations.

Localization at the RMG point – An effective model for the dynamics of a spinon is obtained assuming (2) by considering a chain with an odd number of sites and spinon states $|j\rangle = |\cdots\bullet\!\!-\!\!\bullet\ \bullet\!\!-\!\!\bullet\ \overset{\downarrow}{\bullet}\ \bullet\!\!-\!\!\bullet\ \bullet\cdots\rangle$ with a free spin at site $2j+1$ separating two MG domains. Following the variational approach [11] which consists of projecting $\mathcal{H}$ orthogonally onto the free family of non-orthogonal states $\{|j\rangle\}$, the spinon Hamiltonian reads

$$\mathcal{H}_{\text{spinon}}|j\rangle = \frac{\beta_{2j+1}}{2}\Big(|j-1\rangle + \frac{5}{2}|j\rangle + |j+1\rangle\Big) \ , \qquad (3)$$

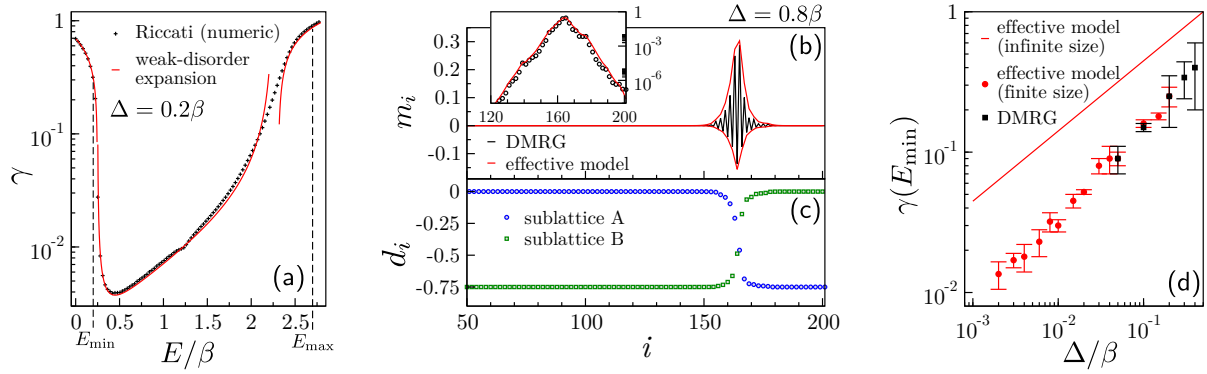

FIG. 1. (color online) *At the RMG point* : (a) Lyapunov exponent γ vs energy E of the effective model. (b) magnetization profile from DMRG in sector $S^z = 1/2$. Inset: log plot. (c) dimerization profile showing the MG domains. (d) finite size effects on the Lyapunov exponent.

in which the MG state energy $E_{\rm MG} = -\frac{3}{4}\sum_i \beta_i$ has been subtracted. Consequently, the motion of the spinon, taking place either on odd or even site sublattices, obeys a special kind of Anderson Hamiltonian expected to induce localization. $\mathcal{H}_{\rm spinon}$ is non-hermitian because $\{|j\rangle\}$ is not orthogonal but this matrix is similar to an hermitian matrix [11]. The spinon wave-function can be written $|\psi_{\rm spinon}\rangle = \sum_j \psi_j |j\rangle$, with coefficients ψ_j. Following the Dyson-Schmidt method [12, 13], we introduce $\tilde\beta_j \equiv \beta_{2j+1}$ and the Riccati variables $R_j = \psi_{j+1}/\psi_j$ to rewrite Schrödinger's equation

$$R_j + 5/2 + 1/R_{j-1} = 2E/\tilde\beta_j \,, \tag{4}$$

for a given spinon energy E. The integrated density of states $N(E)$ and Lyapunov exponent $\gamma(E)$ of a single spinon excitation are obtained by extending the energy to the complex plane. Assuming that the probability density of the Riccati variables converges toward an invariant distribution of measure $dW(R)$ as $j \to \infty$, the characteristic function

$$\Omega(z) = \int dW(R) \ln R \tag{5}$$

is such that $\Omega(E + i0^+) = \gamma(E) + i\pi(1 - N(E))$. These quantities can be obtained either numerically or analytically from a weak-disorder expansion [14] as described below. In the non-disordered case, the spinon dispersion relation is $E(k) = \beta(5/4 + \cos k)$ with k the momentum. By introducing the variables

$$y_j = e^{-2ik}\frac{y_{j-1} - g_j(1 - y_{j-1})}{1 - g_j(1 - y_{j-1})} \,, \tag{6}$$

$$g_j = \frac{(5/4 + \cos k)(\tilde\beta_j - \beta)}{i\tilde\beta_j \sin k} \,, \tag{7}$$

it can be shown that the first term in the expansion in the first moment of the g-distribution gives $\Omega \simeq ik - \overline{g^2}/2$. Specializing to the case of a uniform distribution of width 2Δ, the explicit calculation for energies $E < \beta/4$ gives [11]

$$\gamma(E) = \text{arcosh}\left[\frac{5}{4} - \frac{E}{\beta}\right] - \frac{1}{6}\frac{E^2}{(E - \frac{5}{4}\beta)^2 - \beta^2}\left(\frac{\Delta}{\beta}\right)^2 . \tag{8}$$

The result is compared to numerics on Fig 1(a). In particular, we obtain that the spinon localization length $\xi_{\rm spinon} = 1/\gamma(E_{\rm min})$ in the state with the lowest energy $E_{\rm min} = \beta_{\rm min}/4$ (where $\beta_{\rm min} = \min \tilde\beta_j$), scales as:

$$\xi_{\rm spinon} \simeq \sqrt{2\beta/\Delta} \,. \tag{9}$$

Notice that $\xi_{\rm spinon}$ cannot be captured by RSRG and is not related to the spin correlation length of a MG state.

Another important outcome of the effective model is that it provides hints on the finite-size effects on the spinon energies, with consequences on the spin gap and the localization length. The lowest energy spinon states correspond to the regime of Lifshitz localization, in the tail of the density of states and controlled by a rare-events scenario. Adapting Lifshitz argument [13, 15], a region of length ℓ with many $\tilde\beta_j$ close to $\beta_{\rm min}$ – i.e. provided $|\tilde\beta_j - \beta_{\rm min}| \le C(E_\ell - E_{\rm min})$ for all j in the region, with C a constant – has its lowest energy of the order of $E_\ell \simeq E_{\rm min} + \beta_{\rm min}\pi^2/2\ell^2$, assuming $\beta_{\rm min} > 0$ and writing $E_{\rm min} = \beta_{\rm min}/4$. Since the probability of creating such region scales as $P_\ell \propto [C(E_\ell - E_{\rm min})/2\Delta]^\ell$ for a uniform distribution, the low-energy behavior of the integrated density of states is

$$N(E) \propto \exp\left\{ -\pi\sqrt{\frac{\beta_{\rm min}/2}{E - E_{\rm min}}}\ln\left(\frac{2\Delta/C}{E - E_{\rm min}}\right)\right\} . \tag{10}$$

This behavior is in very good agreement with the numerics on the effective model [11]. Regarding finite-size effects on the spinon energy E_L in a chain of length L, the probability to have the minimum energy must be such that $P_\ell \sim 1/L$. This yields $N(E_L) \sim 1/L$ in Eq. (10), again in good agreement with numerical results [11]. Asymptotically, we thus expect finite-size corrections of the form $E_L \simeq E_{\rm min} + K\beta_{\rm min}(\ln(\ln L)/\ln L)^2$ with K a constant.

In order to validate this effective model, we compare it to accurate DMRG calculations of the magnetization profile in a chain with total spin $S^z = 1/2$. To do so, one relates the local magnetization $m_i \equiv \langle S_i^z\rangle$ to the ψ_j using $m_{2j+1} \simeq \frac{7}{2}|\psi_j|^2$ and $m_{2j} \simeq -2|\psi_j|^2$, assuming that the ψ_j vary smoothly enough. As judged by the results of Fig. 1(b), the effective

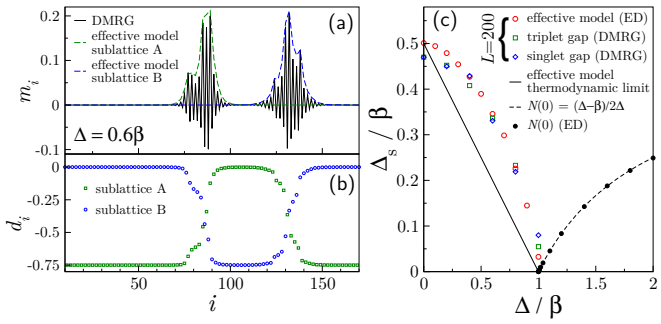

FIG. 2. (Color online) *At the RMG point* – typical magnetization (a) and dimerization (b) profiles in the lowest triplet excited state for $\Delta < \beta$. (c) evolution of the singlet and triplet spin gaps, as well as the spinon density $N(0)$, v.s. the disorder strength Δ.

model provides quantitative predictions of the magnetization profile. From the local dimerization pattern $d_i = \langle \mathbf{S}_i \cdot \mathbf{S}_{i+1} \rangle$ of Fig. 1(c), the localized spinon clearly separates two different MG domains. One can extract the actual ξ_{spinon} from DMRG profiles. On Fig. 1(d), strong deviations between DMRG calculations and the infinite size result (9) are observed. This difference actually originates from finite-size effects : one has to take $\xi_{\text{spinon}} = 1/\gamma(E_L)$ on a finite system, which yields strong deviations, even for large sizes.

Spin gap and transition to a paramagnetic state – From these results on single spinon excitations, we can infer the behavior of the spin gap at the RMG point with increasing disorder. The MG states remain degenerate ground-states at small enough disorder and the lowest triplet excitation above them is to create two localized spinons far away from each other with both the minimal energy E_{min}. They naturally belong to two different sublattices and are expected not to interact on sufficiently large chains. Consequently, the triplet gap, within the effective model approach, is expected to be $\Delta_S = \beta_{\text{min}}/2$ in the thermodynamical limit and degenerate with the singlet gap. We plot in Fig. 2 the evolution of the DMRG triplet and singlet gaps at the RMG point for a box distribution, with increasing Δ. In the clean case, the variational approach slightly overestimates the gap, in particular due to the core interaction between deconfined spinon, and DMRG finds a gap smaller than $\beta/2$. The effective model prediction reads $\Delta_S = (\beta - \Delta)/2$ and vanishes for $\beta = \Delta$, in relatively good agreement with the data. We also give $\Delta_S(L)$ obtained from the effective model to show that DMRG data are essentially controlled by the strong finite-size effects discussed above. Actually, the fact that spinons are localized and thus hardly interact improves the validity of the effective model at intermediate disorder.

Increasing further the disorder strength, E_{min} becomes negative ($E_{\text{min}} = 9\beta_{\text{min}}/4$ for $\beta_{\text{min}} < 0$) so that states with two or more spinons get energetically favored. The MG states are still eigenstates but no longer the ground-states. The resulting picture is a paramagnetic phase of localized spinons, neglecting tiny residual magnetic couplings between spins degree of freedom, provided the spinon density is small enough. The density of spinons in each sublattice is the density of negative energy spinon states $N(0)$. So is the total spinon density. Therefore, the magnetic susceptibility must change from zero to $\chi \sim N(0)$ across the transition. DMRG calculations actually confirm this picture, showing that the ground and first excited states are nearly degenerate states with localized spinons. The order of the quantum phase transition from the gapped to the paramagnetic phase naturally depends on the disorder distribution. The location of the transition, within the effective model picture, is given by $E_{\text{min}} = 0$ and one expects a continuous transition for a continuous disorder distribution. Binary disorder, on the contrary, would yield a first order transition.

In order to determine $N(0)$ for the effective model, one must realize that the Lifshitz argument cannot be used for spinon energies close to zero. Indeed, when $\beta_{\text{min}} \simeq 0$, the energy E_ℓ of a state in a cluster of size ℓ no longer depends on ℓ. Yet, one remarks that the number of negative energy states is actually given by the number of negative $\tilde{\beta}_j$. In the case of a box distribution, one obtains that for $\Delta \geq \beta$:

$$N(0) = (\Delta - \beta)/(2\Delta) \ , \tag{11}$$

and the associated critical exponent of the susceptibility is simply one. Eq. (11) is checked numerically on Fig. 2(c) within the effective model calculations. Checking this law using DMRG is particularly difficult as the spinon density gets very small close to the critical point. Of course, the quantitative predictions from the effective model are to be taken with care because assuming independent spinons requires a low enough spinon density and that neglecting states with non-local dimer is questionable in this regime. In particular, effective magnetic couplings between spinons are non-negligible at high spinon density and the phase is likely to be partially polarized and not strictly speaking paramagnetic.

Away from the RMG point – It is now instructive to turn to the situation where the RMG condition (2) is progressively weaken by uncorrelating the α_i and β_i. This can be done using random variables δ_i, uncorrelated to the β_i, and such that

$$\alpha_i = (1-\lambda)(\beta_i + \beta_{i+1}) + \lambda \delta_i \ , \tag{12}$$

where $\overline{\delta_i} = 2\beta$ and $\lambda \in [0,1]$ is a tuning parameter. The correlations $\overline{\alpha_i \beta_i} - \overline{\alpha_i}\,\overline{\beta_i} = (1-\lambda)\sigma_\beta^2$ (σ^2 denoting a variance) show that the αs and βs get uncorrelated for $\lambda = 1$. As $\sigma_\alpha^2 = 2(1-\lambda)^2\sigma_\beta^2 + \lambda^2\sigma_\delta^2$, we further impose $\sigma_\alpha^2 = 2\sigma_\beta^2$ to study the effect of the correlations only by keeping the disorder strength as for the RMG point. Lastly, using this decoupling, the Hamiltonian (1) nicely splits into two parts with a more transparent physical input :

$$\mathcal{H} = \mathcal{H}_{\text{RMG}} + \lambda \sum_i \eta_i \mathbf{S}_i \cdot \mathbf{S}_{i+1} \ , \tag{13}$$

with $\eta_i = \delta_i - \beta_i - \beta_{i+1}$ for which we have $\overline{\eta_i} = 0$. $\mathcal{H}_{\text{RMG}}$ is the Hamiltonian at the RMG studied above. The second

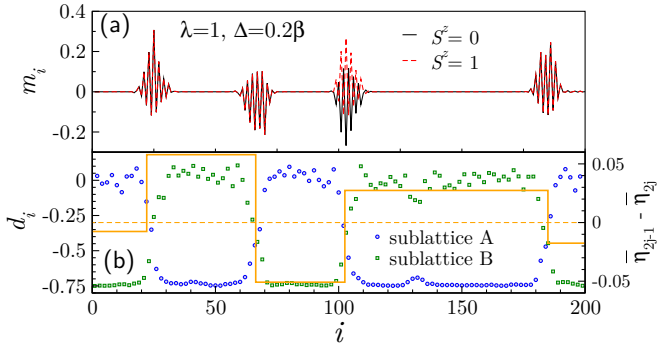

FIG. 3. (Color online) (a) Magnetization profile of a MG chain with uncorrelated couplings displaying localized spinons (b) Dimerization pattern and corresponding average of the random η-dimerization term of Eq. (14) over MG domains (orange line).

term corresponds to a random dimerization term with positive and negative couplings. At small λ, the second term acts as a perturbation which locally lifts the degeneracy between the two MG states of $\mathcal{H}_{\rm RMG}$. Clearly, MG states are no longer eigenstates since high order terms in perturbation theory put weights on states $|i,j\rangle = |$ 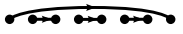 $\rangle$ with a dimer on bond (i,j). More than dressing the MG state, the random dimerization actually destroys the spin gap as soon as $\lambda \neq 0$ and $\sigma_\beta \neq 0$. Indeed, the energy difference $\delta E_{ij} = \langle i,j|\mathcal{H}|i,j\rangle - E_{\rm MG}$ between a long dimer state and the corresponding MG state reads [11]

$$\delta E_{ij} = \frac{3}{4}\big(\beta_{2i-1}+\beta_{2j}\big)+\lambda\Big(\eta_{2j-1}+\sum_{n=i}^{j-1}\eta_{2n-1}-\eta_{2n}\Big). \quad (14)$$

The first part is reminiscent of the spinon localization mechanism induced by $\mathcal{H}_{\rm RMG}$ while the second term can be understood as an effective long range interaction between spinons at i and j stemming from the random dimerization. Then, a rare-event scenario supports the fact that for a infinitely large system, it is always possible to find a region with ηs that do not compensate and such that the random interaction scales as the region size and is negative. Then, since creating two spinons will not cost more than an energy proportional to β, one can make $\delta E_{ij} < 0$ and the spinons localize at the edges of the region (not necessarily in Lifshitz states) with a typical length scale $\xi_{\rm spinon}$ – the region size can be made much larger than $\xi_{\rm spinon}$. As $\xi_{\rm spinon}$ is found to be little affected by λ, we expect that the localization phenomenon remains mostly controlled by $\mathcal{H}_{\rm RMG}$. Physically, the random dimerization locks MG domains to minimize their energy and spinons are localized at their interface. Lastly, as the region can be as large as possible, the effective magnetic coupling between the two spinons is arbitrarily small so that the spin gap vanishes.

This argument is not a mathematical proof of the nature of the small disordered phase. Manipulating superpositions of states with many spinons or long dimers to have quantitative results in this disordered system, as we obtained at the RMG, becomes difficult. In order to support this picture, we performed DMRG calculation for non-zero λ. We do observe that, on a finite-system, the spin gap is strongly reduced by increasing λ, or by increasing Δ at fixed λ. We exhibit in Fig. 3(a) a sample with $\lambda = 1$ where four spinons are present in the ground-state and for which the triplet gap is zero within numerical precision. In a infinite chain, this pattern and similar ones will necessarily appear, making the ground-state gapless. Ferromagnetic couplings between two neighbouring spinons cannot be excluded so that the phase should actually be partially magnetized. The averaged η-dimerization field on Fig. 3(b) supports the locking mechanism of the MG domains. Again, strong finite-size effects prevent us from studying numerically the $\lambda \to 0$ and $\Delta \to 0$ limits without bias.

Comparison with the RSRG approach – The argument developed above, based on localized spinons, is only valid for low enough spinon density, ie. at small disorder. It is interesting to compare these results with the RSRG method best suited to the strong disorder limit. From the RSRG equations given in 11, we notice that the degeneracy of the MG domains at the RMG point translates into an instability in the RSRG procedure. As soon as $\lambda \neq 0$, the gap distribution in the system converges toward an invariant power-law distribution with a non-universal exponent, caracteristic of Griffith phase similar to previous studies [8]. Indeed, due to frustration, the RSRG equations can generate a few effective ferromagnetic couplings, building a large-spin phase [9]. This is in agreement with the low-disorder picture and this partially magnetized phase would extend from infinitely weak to strong disorder continuously. A last remark is that the dimer basis used above for variational calculations has a deep connection with the RSRG picture that tries to catch the most probable dimer configuration from the coupling distribution.

Conclusion – This work provides quantitative results on the interplay between frustration and disorder in random MG chains. We identify two mechanisms at play : the localization of spinons through a non-usual Anderson mechanism and the locking of MG domains by a random dimerization potential. The immediate destruction of the spin gap upon putting disorder is to be contrasted with its robustness for the explicitly dimerized or spin-1 chains which have a non-degenerate ground-state [16]. The presence of degenerate MG states makes the system very sensitive to disorder. We expect the same phenomenogy to play a role in other random VBS. The localization of spinons could also be captured by numerical methods working in the spinon basis [17]. Lastly, this model gives an example of spinons or "free spins" generated by random couplings which could be experimentally relevant and distinct from those generated by vacancies or adatoms.

We thank N. Laflorencie, J.-M. Luck, C. Monthus, C. Sire and C. Texier for insightful discussions. We acknowledge support from grant ANR-2011-BS04-012-01.

* arthur.lavarelo@u-psud.fr

† guillaume.roux@u-psud.fr

[1] C. Majumdar and D. Ghosh, J. Math. Phys. **10**, 1388 (1969); J. Math. Phys. **10**, 1399 (1969).
[2] B. S. Shastry and B. Sutherland, Phys. Rev. Lett. **47**, 964 (1981); W. J. Caspers, K. M. Emmett, and W. Magnus, J. Phys. A: Math. Gen. **17**, 2687 (1984).
[3] T. Senthil, A. Vishwanath, L. Balents, S. Sachdev, and M. P. A. Fisher, Science **303**, 1490 (2004); A. W. Sandvik, Phys. Rev. Lett. **98**, 227202 (2007).
[4] T. Giamarchi, *Quantum Physics in one Dimension* International series of monographs on physics Vol. 121 (Oxford University Press, Oxford, UK, 2004).
[5] S.-k. Ma, C. Dasgupta, and C.-k. Hu, Phys. Rev. Lett. **43**, 1434 (1979); C. Dasgupta and S.-k. Ma, Phys. Rev. B **22**, 1305 (1980); F. Iglói and C. Monthus, Physics Reports **412**, 277 (2005).
[6] D. S. Fisher, Phys. Rev. B **50**, 3799 (1994); Phys. Rev. B **51**, 6411 (1995).
[7] F. Iglói, R. Juhász, and H. Rieger, Phys. Rev. B **61**, 11552 (2000); N. Laflorencie, H. Rieger, A. W. Sandvik, and P. Henelius, Phys. Rev. B **70**, 054430 (2004).
[8] J. A. Hoyos and E. Miranda, Phys. Rev. B **69**, 214411 (2004); C. A. Lamas, D. C. Cabra, M. D. Grynberg, and G. L. Rossini, Phys. Rev. B **74**, 224435 (2006).
[9] E. Westerberg, A. Furusaki, M. Sigrist, and P. A. Lee, Phys. Rev. B **55**, 12578 (1997); K. Yang and R. N. Bhatt, Phys. Rev. Lett. **80**, 4562 (1998).
[10] S. R. White, Phys. Rev. Lett. **69**, 2863 (1992); Phys. Rev. B **48**, 10345 (1993); U. Schollwöck, Rev. Mod. Phys. **77**, 259 (2005).
[11] see supplementary material available online.
[12] F. J. Dyson, Phys. Rev. **92**, 1331 (1953).
[13] J.-M. Luck, *Systèmes désordonnés unidimensionnels*, edited by Cea Saclay (Aléa-Saclay, Gif-sur-Yvette, 1992).
[14] T. M. Nieuwenhuizen, Physica **113A**, 173 (1982); B. Derrida and E. Gardner, J. Phys. (Paris) **45**, 1283 (1984).
[15] I. M. Lifshitz, Soviet Physics Uspekhi **7**, 549 (1965).
[16] R. A. Hyman, K. Yang, R. N. Bhatt, and S. M. Girvin, Phys. Rev. Lett. **76**, 839 (1996); R. A. Hyman and K. Yang, Phys. Rev. Lett. **78**, 1783 (1997); M. Fabrizio and R. Mélin, Phys. Rev. Lett. **78**, 3382 (1997); C. Monthus, O. Golinelli, and T. Jolicœur, Phys. Rev. Lett. **79**, 3254 (1997); C. Monthus, O. Golinelli, and T. Jolicœur, Phys. Rev. B **58**, 805 (1998).
[17] Y. Tang and A. W. Sandvik, Phys. Rev. Lett. **107**, 157201 (2011).

Supplementary material for: Localization of spinons in random Majumdar-Ghosh chains

Non-crossing dimer basis and MG states

We gather some useful results on the non-crossing dimer basis used for variational calculations. The basis is a *free* basis of non-orthogonal states. In the MG physics, the states with dominant weights are rather simple as they are essentially states with nearest-neighbor dimers, with possibly slightly longer dimers locally.

Applying a nearest neighbour term on a MG state :

$$\mathbf{S}_i \cdot \mathbf{S}_{i+1}|\cdots\rangle = \frac{1}{4}|\cdots\rangle + \frac{1}{2}|\cdots\rangle \tag{15}$$

Applying a next-nearest neighbour term on a MG state :

$$\mathbf{S}_i \cdot \mathbf{S}_{i+2}|\cdots\rangle = \frac{1}{4}|\cdots\rangle - \frac{1}{2}|\cdots\rangle, \tag{16}$$

which can be rewritten in the non-crossing dimer basis, using

$$|\cdots\rangle = |\cdots\rangle + |\cdots\rangle. \tag{17}$$

Derivation of the single-spinon effective Hamiltonian

In order to obtain the effective Hamiltonian for the motion of a single spinon, one has to project the Hamiltonian on the variational basis $\{|\cdots\rangle\}$. Applying $\mathbf{S}_i \cdot \mathbf{S}_{i+1}$ on a spinon at position i :

$$\mathbf{S}_i \cdot \mathbf{S}_{i+1}|\cdots\rangle = \frac{1}{4}|\cdots\rangle + \frac{1}{2}|\cdots\rangle \tag{18}$$

Using the following relation

$$|\cdots\rangle = |\cdots\rangle + |\cdots\rangle, \tag{19}$$

one can deduce the application of $\mathbf{S}_i \cdot \mathbf{S}_{i+2}$ in the variational basis :

$$\mathbf{S}_i \cdot \mathbf{S}_{i+2}|\cdots\rangle = -\frac{1}{4}|\cdots\rangle - \frac{1}{2}|\cdots\rangle \tag{20}$$

Applying $\mathbf{S}_{i-1} \cdot \mathbf{S}_{i+1}$ on a spinon at position i :

$$\mathbf{S}_{i-1} \cdot \mathbf{S}_{i+1}|\cdots\rangle = \frac{1}{4}|\cdots\rangle + \frac{1}{2}|\cdots\rangle \tag{21}$$

One can notice that this state is orthogonal to the variational basis. As a result it simply disappears within the variational approach.

Finally, applying the Hamiltonian on a spinon at position i and projecting on the variational basis :

$$\mathcal{H}_{i-1,i,i+1}|\cdots\rangle = \frac{1}{4}(\alpha_i - \beta_{i+1} + \alpha_{i-1} - \beta_{i-1})|\cdots\rangle \tag{22}$$

$$+ \frac{1}{2}(\alpha_i - \beta_{i+1})|\cdots\rangle + \frac{1}{2}(\alpha_{i-1} - \beta_{i-1})|\cdots\rangle \tag{23}$$

Some features of the Majumdar-Ghosh state in the presence of disorder

We discuss some remarkable features of the MG state $|\mathrm{MG}\rangle$ in the presence of disorder. We write α and β the average values of the random couplings and assume that $\alpha = 2\beta$. From (16) and using

$$\langle\cdots|\cdots\rangle = -1/2 \tag{24}$$

and that $\sum_j(\cdots) \to \frac{L}{2}\overline{(\cdots)}$ for large enough system

$$\langle \mathrm{MG}|\mathcal{H}|\mathrm{MG}\rangle = E_{\mathrm{MG}} = -\frac{3}{4}\sum_{j=1}^{L/2}\alpha_{2j-1} \to -\frac{3}{4}L\beta\ . \tag{25}$$

Notice that the above energy is exact even when (2) is not satisfied, but that the simplification from averaging only comes with the thermodynamic limit. In particular, it is remarkable that the energy remains independent of the disorder strength Δ. The fact that the MG state is not an eigenstate in general (when (2) is not satisfied) can be captured by calculating the energy dispersion of the state:

$$\sigma^2_{\mathrm{MG}} \equiv \langle \mathrm{MG}|\mathcal{H}^2|\mathrm{MG}\rangle - E^2_{\mathrm{MG}} \to \frac{3L}{16}\left[\sigma^2_\alpha + 2\sigma^2_\beta + 2\alpha^2 + 8\beta^2 - 4(\overline{\alpha\beta} + \alpha\beta)\right] \tag{26}$$

On can check on this expression that we do have $\sigma_{\mathrm{MG}} = 0$ when (2) is fulfilled, as expected for an eigenstate.

Energy of a long dimer state

We denote $|i,j\rangle = |\cdots$ 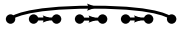 $\cdots\rangle$, the singlet product state with a long dimer between sites $2i-1$ and $2j$ ($i \leqslant j$). This state can be seen as a singlet state between two localized spinons. So, away from MG line ($\lambda > 0$), it may have a lower energy than the MG state. Let us apply the Hamiltonian on this state :

$$\begin{aligned}
\mathcal{H}|i,j\rangle =& \frac{1}{4}\left(-3\sum_{n=1}^{i-1}\alpha_{2n-1} + \sum_{n=1}^{i-2}(\alpha_{2n} - \beta_{2n} - \beta_{2n+1})\right)|i,j\rangle \\
&+\frac{1}{2}\sum_{n=1}^{i-2}(\alpha_{2n} - \beta_{2n} - \beta_{2n+1})|\cdots \text{ 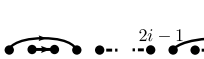 \cdots\rangle \\
&+\frac{1}{4}\left(-3\sum_{n=i}^{j-1}\alpha_{2n} + \sum_{n=i+1}^{j-1}(\alpha_{2n-1} - \beta_{2n-1} - \beta_{2n})\right)|i,j\rangle \\
&+\frac{1}{2}\sum_{n=i+1}^{j-1}(\alpha_{2n-1} - \beta_{2n-1} - \beta_{2n})|\cdots \text{ \cdots\rangle \\
&+\frac{1}{4}\left(-3\sum_{n=j+1}^{\frac{L}{2}}\alpha_{2n-1} + \sum_{n=j+1}^{\frac{L}{2}-1}(\alpha_{2n} - \beta_{2n} - \beta_{2n+1})\right)|i,j\rangle \\
&+\frac{1}{2}\sum_{n=j+1}^{\frac{L}{2}-1}(\alpha_{2n} - \beta_{2n} - \beta_{2n+1})|\cdots \text{ \cdots\rangle \\
&+\frac{1}{4}(\alpha_{2i-2} + \alpha_{2i-1} - \beta_{2i-2} - \beta_{2i} + \alpha_{2i-1} + \alpha_{2j} - \beta_{2i-1} - \beta_{2j+1})|i,j\rangle \\
&+\frac{1}{2}\left[(\alpha_{2i-2} - \beta_{2i-2})|i-1,j\rangle + \frac{1}{2}(\alpha_{2i-1} - \beta_{2i})|i+1,j\rangle + (\alpha_{2j-1} - \beta_{2j-1})|i,j-1\rangle + (\alpha_{2j} - \beta_{2j+1})|i,j+1\rangle\right] \\
&+\frac{1}{4}(\beta_{2i-1} + \beta_{2j})|i,j\rangle + \frac{1}{2}\left[\beta_{2i-1}|\cdots \text{ \cdots\rangle + \beta_{2j}|\cdots \text{ \cdots\rangle\right]\ .
\end{aligned}$$

Of course, this state is not exactly an eigenstate but using

$$\langle i,j|i\pm 1,j\rangle = \langle i,j|i,j\pm 1\rangle = -\frac{1}{2}, \tag{27}$$

one can calculate its energy :

$$\langle i,j|\mathcal{H}|i,j\rangle = -\frac{3}{4}\Big(\sum_{n=1}^{i-1}\alpha_{2n-1} + \sum_{n=i}^{j-1}\alpha_{2n} + \sum_{n=j+1}^{L/2}\alpha_{2n-1}\Big)\ , \tag{28}$$

and compare it with the energy of the MG state :

$$\langle i,j|\mathcal{H}|i,j\rangle - \langle \mathrm{MG}|\mathcal{H}|\mathrm{MG}\rangle = \frac{3}{4}\Big(\sum_{n=i}^{j}\alpha_{2n-1} - \sum_{n=i}^{j-1}\alpha_{2n}\Big) = \frac{3}{4}\big(\beta_{2i-1}+\beta_{2j}\big) + \lambda\Big(\eta_{2j-1} + \sum_{n=i}^{j-1}\eta_{2n-1} - \eta_{2n}\Big)\,. \tag{29}$$

We recall that the ηs variables have a mean value $\overline{\eta}=0$ and variance

$$\sigma_\eta^2 = 4\frac{1-\lambda}{\lambda}\sigma_\beta^2 \tag{30}$$

Effective model

Similarity to a symmetric matrix

The effective model of Eq. (3) is in a non-hermitian form due to the non-orthogonal nature of the dimer basis. The associated matrix simply reads (writing $s=5/2$):

$$H = \frac{1}{2}\begin{pmatrix} s\beta_1 & \beta_1 & & & \\ \beta_2 & s\beta_2 & \beta_2 & & \\ & \beta_3 & s\beta_3 & \beta_3 & \\ & & \beta_4 & s\beta_4 & \ddots \\ & & & \ddots & \ddots \end{pmatrix}\,. \tag{31}$$

When all the βs are positive numbers, using the similarity transform diagonal matrix $D=\mathrm{diag}(\sqrt{\beta_1},\sqrt{\beta_2},\ldots)$ puts H into the following tridiagonal symmetric form

$$D^{-1}HD = \frac{1}{2}\begin{pmatrix} s\beta_1 & \sqrt{\beta_1\beta_2} & & & \\ \sqrt{\beta_1\beta_2} & s\beta_2 & \sqrt{\beta_2\beta_3} & & \\ & \sqrt{\beta_2\beta_3} & s\beta_3 & \sqrt{\beta_3\beta_4} & \\ & & \sqrt{\beta_3\beta_4} & s\beta_4 & \ddots \\ & & & \ddots & \ddots \end{pmatrix}\,. \tag{32}$$

clearly showing that all eigenvalues are real, as for the eigenvectors.

When some of the βs are negative, applying the same transform then leads to a complex symmetric matrix, but not to an hermitian matrix. A non-diagonal similarity transform is then required. Looking at the 2×2 and 3×3 cases shows that it becomes pretty difficult to construct a similarity transform matrix. In addition to showing that the eigenvalues are all real, finding such transform would have been very useful to get numerically the spectrum for very large systems. Still, we numerically observe and expect that all the eigenvalues and ψ_j coefficients are real since the effective Hamiltonian stems from an initially hermitian Hamiltonian.

Weak-coupling results

We gather the weak-coupling results on the Lyapunov exponent of the effective model. The energy is parametrized through the variables t or k:

- for $E<\frac{\beta}{4}$ and $E=\beta(\frac{5}{4}-\cosh t)$: $\quad \gamma = t - \frac{1}{6}\left(\frac{(\frac{5}{4}-\cosh t)\Delta}{\sinh(t)\beta}\right)^2$
- for $\frac{\beta}{4}<E<\frac{9\beta}{4}$ and $E=\beta(\frac{5}{4}+\cos k)$: $\quad \gamma = \frac{1}{6}\left(\frac{(\frac{5}{4}+\cos k)\Delta}{\sin(k)\beta}\right)^2$
- for $E>\frac{9\beta}{4}$ and $E=\beta(\frac{5}{4}+\cosh t)$: $\quad \gamma = t - \frac{1}{6}\left(\frac{(\frac{5}{4}+\cosh t)\Delta}{\sinh(t)\beta}\right)^2$

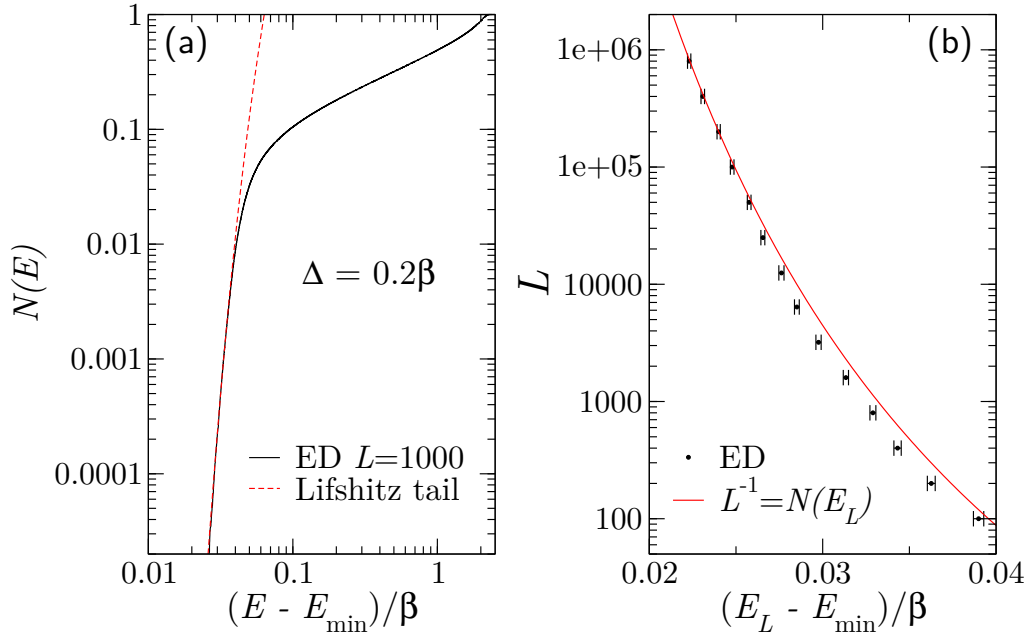

FIG. 4. (Color online) (a) Integrated density of states at low-energies compared with Lifshitz argument od Eq. (10). (b) Finite-size effects on the spinon energy.

Numerics on the Lifshitz tail

We give in Fig. 4(a-b) the comparison between numerical calculations on the effective model and finite-size corrections obtained from Lifshitz argument.

A wrong argument for the susceptibility exponent at the random MG point

A naive argument for $\beta_{\rm min} < 0$ is the following : the susceptibility χ of the paramagnetic phase should correspond to independently filling spinons in single-spinon *Lifshitz states* up to zero energy. One is tempted to use a Lifshitz formula for $N(0)$, which is similar to (10) with the changes $E_\ell \simeq E_{\rm min} - \beta_{\rm min}\pi^2/2\ell^2$ and $E_{\rm min} = 9\beta_{\rm min}/4$. Using $\beta_{\rm min} = \Delta_c - \Delta$, with $\Delta_c = \beta$ the critical disorder strength, one gets for the susceptibility exponent $\phi = \pi\sqrt{2}/3 \simeq 1.481$ for the uniform distribution. Actually, such a prediction is wrong for the reason that the Lifshitz formula does not work close to the $E = 0$ while it does work close to $E_{\rm min}$. This behavior is true whatever the smallness of the disorder strength. Instead, we observe that $N(E)$ is linear close to $E = 0$ and that $N(0)$ is rather linear with $\Delta - \Delta_c$. As discussed in the main text, the correct $N(0)$ is obtained by coupling the number of negative βs which leads to $\phi = 1$ for the uniform distribution.

On the convergence of DMRG calculations

DMRG calculations were performed using the finite-size algorithm, targeting one or two states (for instance to determine the singlet gap) and keeping typically from 400 to 1000 kept states. As MG are products of dimers, they have a simple matrix-product form which makes DMRG pretty efficient. The energies are converged to high precision. In the presence of localized spinons and in the $S^z = 0$ sector, the local magnetization should be zero everywhere. Yet, DMRG builds up a variational states with non-zero magnetization at the place of localized spinons. Indeed, due to the localization of spinons, triplet and singlet states are degenerate within an energy gap that is tiny (we observed gaps below $10^{-8}\beta$) and controlled by the residual magnetic couplings between spinons. Thus, the effective couplings between spinons become so tiny that it is extremely hard for DMRG to differentiate between the singlet or $S^z = 0$ triplet state and gives a superposition of these states as an output, with a finite local magnetization. Still, the spinon localization and magnetization profiles in the $S^z = 1$ are very well converged.

RSRG equations for the dimerized chain

Due to frustration, ferromagnetic couplings can be generated during the RSRG scheme so one has to take into account the possibility to generate spins higher than 1/2. The renormalized couplings, which are here written in the general form J_{ij}, depend on the spin size s_i. We have the following two equations corresponding to the decimation scheme sketched in Fig. 5:

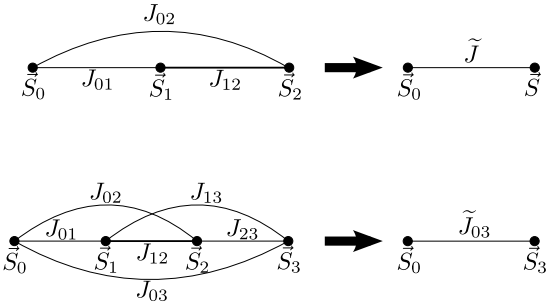

FIG. 5. Decimation scheme for the RSRG procedure of Model (1).

- if $s_1 \neq s_2$ or $J_{12} < 0$, we take $s = s_1 + s_2$ for $J_{12} < 0$ and $s = |s_1 - s_2|$ for $J_{12} > 0$ and we have

$$\widetilde{J} = \frac{s(s+1) + s_1(s_1+1) - s_2(s_2+1)}{2s(s+1)} J_{01} + \frac{s(s+1) + s_2(s_2+1) - s_1(s_1+1)}{2s(s+1)} J_{02} \tag{33}$$

- if $s_1 = s_2$ and $J_{12} > 0$, we have

$$\widetilde{J}_{03} = J_{03} + \frac{2}{3} s_1(s_1+1) \frac{(J_{01} - J_{02})(J_{23} - J_{13})}{J_{12}} \tag{34}$$

In particular for the first decimations, if α_i is the strongest coupling, spins i and $i+1$ are decimated and the renormalized couplings between remaining spins are :

$$\widetilde{J}_{i-1,i+2} = \frac{(\alpha_{i-1} - \beta_i)(\alpha_{i+1} - \beta_{i+1})}{2\alpha_i} = \frac{(\beta_{i-1} + \lambda\eta_{i-1})(\beta_{i+2} + \lambda\eta_{i+1})}{2\alpha_i} \tag{35}$$

$$\widetilde{J}_{i-2,i+2} = \frac{\beta_{i-1}(\alpha_{i+1} - \beta_{i+1})}{2\alpha_i} = \frac{\beta_{i-1}(\beta_{i+2} + \lambda\eta_{i+1})}{2\alpha_i} \tag{36}$$

$$\widetilde{J}_{i-1,i+3} = \frac{(\alpha_{i-1} - \beta_i)\beta_{i+2}}{2\alpha_i} = \frac{(\beta_{i-1} + \lambda\eta_{i-1})\beta_{i+2}}{2\alpha_i} \tag{37}$$

$$\widetilde{J}_{i-2,i+3} = \frac{\beta_{i-1}\beta_{i+2}}{2\alpha_i} \tag{38}$$

Thus for $\lambda = 0$, we end up with four degenerated couplings, implicitly reminiscent of the degeneracy of the MG domains at the RMG point, which makes the continuation of the RSRG procedure unstable numerically and ill-posed.

We have studied the behavior of the RSRG equations which lead to a large-spin Griffith phase but the details will be published elsewhere.


$2i-1$
$2j$